Chiral-odd generalized parton distributions of sea quarks at $\xi = 0$ in the light-cone quark model

Xiaoyan Luan and Zhun Lu*

School of Physics, Southeast University, Nanjing 211189, China

(Received 30 April 2024; accepted 15 July 2024; published 14 August 2024)

We study the chiral-odd generalized parton distributions (GPDs) of the $\bar{u}$ and $\bar{d}$ quarks inside the proton at zero skewness using the overlap representation within the light-cone formalism. Utilizing the light-cone wave functions of the proton obtained from the baryon-meson fluctuation model in terms of the $|q\bar{q}B\rangle$ Fock states, we provide expressions for the GPDs $\tilde{H}_T^{\bar{q}/P}(x,0,t)$, $H_T^{\bar{q}/P}(x,0,t)$, and $E_T^{\bar{q}/P}(x,0,t)$ where $\bar{q} = \bar{u}$ and $\bar{d}$. Numerical results for these GPDs in momentum space as well as in impact parameter space are presented. Additionally, we investigate specific combinations of the chiral-odd GPDs in impact parameter space, focusing on the spin-orbit correlation effect of the sea quarks.

DOI: 10.1103/PhysRevD.110.034021

I. INTRODUCTION

Understanding the internal structure of hadrons in terms of constituent quarks, gluon, and sea quarks is one of the main goals of QCD and hadronic physics. Generalized parton distributions (GPDs) [1–4], viewed as the extension of the standard parton distribution functions (PDFs), are crucial for describing the three-dimensional structure of nucleons complementary to the transverse momentum-dependent parton distributions. The GPDs correspond to off-forward matrix elements of nonlocal operators, accessible experimentally through deeply virtual Compton scattering (DVCS) [2,5,6] or deeply virtual meson production [7–10]. At leading twist, there are eight GPDs: four chiral-even (helicity-nonflip) GPDs H, E, $\tilde{H}$, $\tilde{E}$ and four chiral-odd (helicity-flip) GPDs H_T, E_T, $\tilde{H}_T$, $\tilde{E}_T$. The GPDs depend on three independent kinematic variables, the longitudinal momentum faction x of the parton, the square of the total momentum transferred t, and the longitudinal momentum transferred skewness ξ. In the forward limit, H, $\tilde{H}$, H_T reduce to the usual unpolarized distribution, helicity distribution, and transversity distribution, respectively. On the one hand, the chiral-even GPDs encode richer knowledge on the orbital angular momentum (OAM) of quarks inside the nucleon [2,3,11,12], and electromagnetic and gravitational form factors [13,14], as well as charge and magnetization densities [15–19]. On the other hand, the chiral-odd GPDs are sources of the correlation between the spin and OAM carried by quarks inside the nucleon [20,21]. Thus, they contain a wealth of information about the partonic structure of the hadron. Through Fourier transform with respect to the transverse momentum transfer $\mathbf{\Delta}_T$, one can obtain the distributions in the impact parameter space that provide tomographic description of the nucleon structure. Particularly, the impact-parameter-dependent GPDs have a probabilistic interpretation and satisfy the positivity condition [22,23].

In recent years, extensive experimental and theoretical studies on GPDs have been conducted. Experimental data from hard exclusive scattering have been collected by collaborations such as H1 [24–26], ZEUS [27,28], HERMES [29–31], COMPASS [32], and JLab [33]. Chiral-even GPDs are accessible in exclusive processes like DVCS [2,5,6] and hard exclusive meson production [34,35] through factorization theorems. In contrast, measuring chiral-odd GPDs is challenging due to their helicity-flip nature, requiring combination with another chiral-odd object in the amplitude to avoid decoupling in most hard processes. At present, it is proposed that they can be accessed through deeply virtual pseudoscalar meson production processes sensitive to chiral-odd GPDs [10,36,37], such as photon production of vector meson [38] and diffractive double meson production [39–41]. Recent COMPASS measurements [42] on exclusive ρ^0 muon production by scattering muons off the transversely polarized proton showed a nonzero single-spin asymmetry $A_{UT}^{\sin\phi_S}$, well described by a GPD-based model [43] using the handbag approach, which is interpreted as the first evidence for the existence of chiral-odd GPDs, especially the transversity GPD H_T. Theoretical studies of hard exclusive pseudoscalar meson electroproduction [10,44–47], like π^0

*Contact author: zhunlu@seu.edu.cn

and η electroproduction [10,36,37,44,48–51], indicate strong contributions from transversely polarized virtual photons necessitating the inclusion of transversity GPDs alongside chiral-even GPDs. Notably, simulations for the leading-twist contributions in the $\gamma\rho$ photoproduction process from chiral-odd GPDs [38,52–54] are underway at the kinematics of the future Electron-Ion Collider.

Various model calculations have explored chiral-odd GPDs. Early calculations in the bag model found H_T is nonzero [55]. In Refs. [56,57], the chiral-odd GPDs at nonzero skewness have been studied in a constituent quark model using the overlap representation in terms of light-cone wave functions (LCWFs). In Ref. [58], the authors investigated the chiral-odd GPDs for both zero and nonzero skewness in the light-front quark-diquark model motivated by the soft-wall anti–de Sitter QCD. The general properties of the chiral-odd GPDs have been investigated in transverse and longitudinal impact parameter spaces in Ref. [59]. The impact parameter representation of the GPDs also has been studied in a QED model of a dressed electron [60] and in a quark-diquark model [61] at zero skewness. In Refs. [44,62], the chiral-odd GPDs were studied through a physically motivated parametrization based on the Reggenized diquark model. The information about the Mellin moments of chiral-odd GPDs has also been obtained through lattice QCD [63–68]. However, most of those model calculations focus on valence quarks; the knowledge of the sea quark Chiral-odd GPDs in a proton is still limited.

In this paper, we apply the light-cone quark model to calculate the chiral-odd GPDs H_T, E_T, $\tilde{H}_T$, and $\tilde{E}_T$ of the $\bar{u}$ and $\bar{d}$ quarks at zero skewness using the overlap representation. Then we calculate the chiral-odd GPDs of the sea quarks at $\xi = 0$ where $\tilde{E}_T$ does not contribute, since it is an odd function of ξ. To generate the sea quark degree of freedom, we adopt the assumption proposed in Ref. [69] that the proton can fluctuate to a composite state containing a meson M and a baryon B, and $q\bar{q}$ are components of the pion meson; the LCWFs of the proton can be derived in terms of the $|q\bar{q}B\rangle$ Fock states, which have been calculated in Ref. [70]. In this framework, the chiral-odd GPDs of $\bar{u}$ and $\bar{d}$ can be obtained using these LCWFs. Fourier transforming with respect to $\mathbf{\Delta}_T$, the chiral-odd GPDs $H^{\bar{q}/P}$, $E^{\bar{q}/P}$, $\tilde{H}^{\bar{q}/P}$ in impact parameter space are also given. Using these results, we present numerical results for specific combinations of the chiral-odd GPDs $\mathcal{H}_T - \frac{\Delta_b}{4m^2}\tilde{\mathcal{H}}_T$, $\mathcal{E}_T + 2\tilde{\mathcal{H}}_T$, and $\epsilon_{ij} b_j \frac{\partial}{\partial B}(\mathcal{E}_T + 2\tilde{\mathcal{H}}_T)$.

The paper is organized as follows. In Sec. II, we derive the overlap representation in terms of LCWFs of the pion and kaon mesons. In Sec. III, we apply LCWFs to calculate the chiral-odd GPDs of sea quarks. In Sec. IV, we present the numerical results of these GPDs in momentum as well as impact parameter space. We summarize the paper in Sec. V.

II. CHIRAL-ODD GPDS IN OVERLAP REPRESENTATION

The GPDs can be defined as the off-forward matrix elements of the quark-quark proton correlator function on the light cone,

$$F^{\Gamma}_{\Lambda',\Lambda}(x,\xi,t) = \frac{1}{2}\int \frac{dz^-}{2\pi} e^{ix\bar{P}^+ z^-} \left\langle p',\Lambda' \middle| \bar{\psi}\left(-\frac{z}{2}\right)\Gamma\psi\left(\frac{z}{2}\right) \middle| p,\Lambda \right\rangle \Big|_{z^+=0,\mathbf{z}_T=0}, \tag{1}$$

where Γ is the Dirac matrix chosen from $\gamma^+, \gamma^+\gamma_5, i\sigma^{i+}\gamma_5$ $(i = 1, 2)$, and Λ, Λ' denote the target helicities in the initial and final states.

For the chiral-odd case where $\Gamma = i\sigma^{i+}\gamma_5$, $F^{i\sigma^{i+}\gamma_5}_{\Lambda',\Lambda}$ can be parametrized as [71]

$$\begin{aligned} F^{[i\sigma^{i+}\gamma^5]}_{\Lambda'\Lambda} &= \frac{i\epsilon^{ij}}{2P^+}\bar{U}(p',\Lambda')\left[i\sigma^{+j}H_T + \frac{\gamma^+\Delta^j - \Delta^+\gamma^j}{2M}E_T + \frac{P^+\Delta^j}{M^2}\tilde{H}_T - \frac{P^+\gamma^j}{M}\tilde{E}_T\right]U(p,\Lambda) \\ &= \left[\frac{i\epsilon^{ij}\Delta^j}{2M}\left(E_T + 2\tilde{H}_T\right) + \frac{\Lambda\Delta^i}{2M}\left(\tilde{E}_T - \xi E_T\right)\right]\delta_{\Lambda'\Lambda} + \left[(\delta_{i1} + i\Lambda\delta_{i2})H_T - \frac{i\epsilon^{ij}\Delta^j(\Lambda\Delta^1 + i\Delta^2)}{2M^2}\tilde{H}_T\right]\delta_{-\Lambda'\Lambda}. \end{aligned} \tag{2}$$

Here, ϵ^{ij} is the antisymmetric tensor with $\epsilon^{12} = -\epsilon^{21} = 1$, $P = (p + p')/2$ is the average proton momentum, $\Delta = p' - p$ is the momentum transfer to the proton with $t = \Delta^2 = -\Delta_T^2$, and $\xi = -\Delta^+/2P^+$ is the skewness parameter.

We use $\uparrow$ ($\downarrow$) to denote the positive (negative) helicity of the proton. For $i = 1$, we have

$$F^1_{\uparrow\uparrow} = \frac{i\Delta_2}{2M}(2\tilde{H}_T + E_T) + \frac{\Delta_1}{2M}(\tilde{E}_T - \xi E_T), \qquad F^1_{\downarrow\downarrow} = \frac{i\Delta_2}{2M}(2\tilde{H}_T + E_T) - \frac{\Delta_1}{2M}(\tilde{E}_T - \xi E_T), \tag{3}$$

$$F^1_{\uparrow\downarrow} = H_T + \frac{\tilde{H}_T}{2M^2}(-i\Delta_2)(-\Delta_1 + i\Delta_2), \qquad F^1_{\downarrow\uparrow} = H_T + \frac{\tilde{H}_T}{2M^2}(-i\Delta_2)(\Delta_1 + i\Delta_2). \tag{4}$$

And for $i = 2$, we have

$$F^2_{\uparrow\uparrow} = \frac{-i\Delta_1}{2M}(2\tilde{H}_T + E_T) + \frac{\Delta_2}{2M}(\tilde{E}_T - \xi E_T), \qquad F^2_{\downarrow\downarrow} = \frac{-i\Delta_1}{2M}(2\tilde{H}_T + E_T) - \frac{\Delta_2}{2M}(\tilde{E}_T - \xi E_T), \tag{5}$$

$$F^2_{\uparrow\downarrow} = -iH_T + \frac{\tilde{H}_T}{2M^2}(i\Delta_1)(-\Delta_1 + i\Delta_2), \qquad F^2_{\downarrow\uparrow} = iH_T + \frac{\tilde{H}_T}{2M^2}(i\Delta_1)(\Delta_1 + i\Delta_2). \tag{6}$$

Using Eqs. (3)–(6), the chiral-odd GPDs can be obtained from the following combinations:

$$\frac{i\Delta_1\Delta_2}{M^2}\tilde{H}_T = \frac{F^1_{\uparrow\downarrow} - F^1_{\downarrow\uparrow}}{2} - \frac{i(F^2_{\uparrow\downarrow} + F^2_{\downarrow\uparrow})}{2}, \tag{7}$$

$$2H_T + \frac{\Delta_T^2}{2M^2}\tilde{H}_T = \frac{F^1_{\uparrow\downarrow} + F^1_{\downarrow\uparrow}}{2} + \frac{i(F^2_{\uparrow\downarrow} - F^2_{\downarrow\uparrow})}{2}, \tag{8}$$

$$\frac{\Delta_1 + i\Delta_2}{2M}(\tilde{E}_T - \xi E_T) = \frac{F^1_{\uparrow\uparrow} - F^1_{\downarrow\downarrow}}{2} + \frac{i(F^2_{\uparrow\uparrow} - F^2_{\downarrow\downarrow})}{2}, \tag{9}$$

$$\frac{\Delta_1 + i\Delta_2}{2M}(2\tilde{H}_T + E_T) = \frac{F^1_{\uparrow\uparrow} + F^1_{\downarrow\downarrow}}{2} + \frac{i(F^2_{\uparrow\uparrow} + F^2_{\downarrow\downarrow})}{2}. \tag{10}$$

According to Ref. [72], GPDs can be related to the following matrix elements:

$$A_{\Lambda'\mu',\Lambda\mu} = \int \frac{dz^-}{2\pi} e^{ixP^+z^-} \langle p', \Lambda' | \mathcal{O}_{\mu',\mu}(z) | p, \Lambda \rangle \Big|_{z^+=0,\mathbf{z}_T=0}, \tag{11}$$

where μ' and μ denote the helicities of the active parton. The operators $\mathcal{O}_{\mu',\mu}$ in the definitions of the quark distributions have been given in Ref. [72].

Similarly, for antiquark there is

$$\mathcal{O}_{-,+} = \frac{i}{4}\psi\sigma^{+1}(1-\gamma_5)\bar{\psi} = -\frac{i}{4}\bar{\psi}\sigma^{+1}(1-\gamma_5)\psi, \tag{12}$$

$$\mathcal{O}_{+,-} = -\frac{i}{4}\psi\sigma^{+1}(1+\gamma_5)\bar{\psi} = \frac{i}{4}\bar{\psi}\sigma^{+1}(1+\gamma_5)\psi. \tag{13}$$

Here, $+(-)$ denotes the positive (negative) helicity of the antiquark, which is different from the case for the antiquark in Ref. [20] where $+(-)$ denotes the quark helicity. Compared to the case of quarks, there is a global negative sign in the case of antiquarks because the order of the operators $\bar{\psi}$ and ψ has to be reversed to obtain a density operator for antiquarks. The correlation functions in Eq. (2) thus can be written in terms of the antiquark-proton helicity amplitudes as

$$F^1_{\Lambda'\Lambda} = -(A_{\Lambda'+,\Lambda-} + A_{\Lambda'-,\Lambda+}), \tag{14}$$

$$F^2_{\Lambda'\Lambda} = i(A_{\Lambda'-,\Lambda+} - A_{\Lambda'+,\Lambda-}). \tag{15}$$

Here, the relation $\sigma^{i+} = -\epsilon^{ij} i\sigma^{j+}\gamma_5$ is used.

Within the light-cone approach, the Fock-state expansion for a proton is expressed as

$$|p, \Lambda\rangle = \sum_n \prod_{i=1}^n \frac{\mathrm{d}x_i \mathrm{d}^2 k^i_\perp}{\sqrt{x_i} 16\pi^3} 16\pi^3 \delta\Big(1 - \sum_j x_j\Big) \delta^2\Big(\sum_{j=1}^n k^j_\perp\Big) \psi_n(x_i, k^i_\perp, \lambda_i) |n; x_i p^+, x_i p_\perp + k^i_\perp, \lambda_i\rangle.$$

Similar to the case of chiral-even GPDs [73], there are also contributions from the $n \to n$ diagonal overlap in the kinematical regions $\xi < x < 1$ and $\xi - 1 < x < 0$. Therefore, Eq. (2) can be expressed through the overlap representation in terms of the LCWFs as follows [59]:

$$F^1_{\Lambda'\Lambda} = -(1-\xi)^{(1-\frac{n}{2})} \sum_{\lambda_i, n} \int \prod_{i=1}^n \frac{dx_i d^2 k^i_\perp}{16\pi^3} 16\pi^3 \delta\Big(1 - \sum_j x_j\Big) \delta^2\Big(\sum_{j=1}^n k^j_\perp\Big) \delta(x - x_1) \times \psi_n^{\Lambda'*}(x'_i, k'^i_\perp, \lambda'_i) \psi_n^{\Lambda}(x_i, k^i_\perp, \lambda_i) \delta_{\lambda'_1, -\lambda_1} [\delta_{\lambda'_i, \lambda_i}(i = 2 \ldots n)], \tag{16}$$

$$F^2_{\Lambda'\Lambda} = i(1-\xi)^{(1-\frac{n}{2})} \sum_{\lambda_i, n} \int \prod_{i=1}^n \frac{dx_i d^2 k^i_\perp}{16\pi^3} 16\pi^3 \delta\Big(1 - \sum_j x_j\Big) \delta^2\Big(\sum_{j=1}^n k^j_\perp\Big) \delta(x - x_1) \times \mathrm{sign}(\lambda_1) \psi_n^{\Lambda'*}(x'_i, k'^i_\perp, \lambda'_i) \psi_n^{\Lambda}(x_i, k^i_\perp, \lambda_i) \delta_{\lambda'_1, -\lambda_1} [\delta_{\lambda'_i, \lambda_i}(i = 2 \ldots n)], \tag{17}$$

where $\lambda_1(\lambda_1')$ represents the helicity of the initial (final) struck antiquark, and $\lambda_i(\lambda_i')$ denotes the helicity of the initial (final) spectators.

We thus obtain the formulas for the chiral-odd GPDs within the overlap representation in terms of the proton LCWFs,

$$\frac{i\Delta_1\Delta_2}{M^2}\tilde{H}_T(x,\xi,t) = -(1-\xi)^{(1-\frac{n}{2})}\sum_{\lambda_i,n}\int\prod_{i=1}^{n}\frac{dx_i d^2k_\perp^i}{16\pi^3}16\pi^3\delta\left(1-\sum_j x_j\right)\delta^2\left(\sum_{j=1}^{n}k_\perp^j\right)\delta(x-x_1) \times\left[\psi_{+n}^{\uparrow *}(x_i',k_\perp'^i,\lambda_i')\psi_{-n}^{\downarrow}(x_i,k_\perp^i,\lambda_i)-\psi_{-n}^{\downarrow *}(x_i',k_\perp'^i,\lambda_i')\psi_{+n}^{\uparrow}(x_i,k_\perp^i,\lambda_i)\right][\delta_{\lambda_i',\lambda_i}(i=2\ldots n)], \tag{18}$$

$$2H_T+\frac{\Delta_T^2}{2M^2}\tilde{H}_T(x,\xi,t) = -(1-\xi)^{(1-\frac{n}{2})}\sum_{\lambda_i,n}\int\prod_{i=1}^{n}\frac{dx_i d^2k_\perp^i}{16\pi^3}16\pi^3\delta\left(1-\sum_j x_j\right)\delta^2\left(\sum_{j=1}^{n}k_\perp^j\right)\delta(x-x_1) \times\left[\psi_{-n}^{\uparrow *}(x_i',k_\perp'^i,\lambda_i')\psi_{+n}^{\downarrow}(x_i,k_\perp^i,\lambda_i)+\psi_{+n}^{\downarrow *}(x_i',k_\perp'^i,\lambda_i')\psi_{-n}^{\uparrow}(x_i,k_\perp^i,\lambda_i)\right][\delta_{\lambda_i',\lambda_i}(i=2\ldots n)], \tag{19}$$

$$\frac{\Delta_1+i\Delta_2}{2M}(\tilde{E}_T-\xi E_T)(x,\xi,t) = -(1-\xi)^{(1-\frac{n}{2})}\sum_{\lambda_i,n}\int\prod_{i=1}^{n}\frac{dx_i d^2k_\perp^i}{16\pi^3}16\pi^3\delta\left(1-\sum_j x_j\right)\delta^2\left(\sum_{j=1}^{n}k_\perp^j\right)\delta(x-x_1) \times\left[\psi_{-n}^{\uparrow *}(x_i',k_\perp'^i,\lambda_i')\psi_{+n}^{\uparrow}(x_i,k_\perp^i,\lambda_i)-\psi_{-n}^{\downarrow *}(x_i',k_\perp'^i,\lambda_i')\psi_{+n}^{\downarrow}(x_i,k_\perp^i,\lambda_i)\right][\delta_{\lambda_i',\lambda_i}(i=2\ldots n)], \tag{20}$$

$$\frac{\Delta_1+i\Delta_2}{2M}(2\tilde{H}_T+E_T)(x,\xi,t) = -(1-\xi)^{(1-\frac{n}{2})}\sum_{\lambda_i,n}\int\prod_{i=1}^{n}\frac{dx_i d^2k_\perp^i}{16\pi^3}16\pi^3\delta\left(1-\sum_j x_j\right)\delta^2\left(\sum_{j=1}^{n}k_\perp^j\right)\delta(x-x_1) \times\left[\psi_{-n}^{\uparrow *}(x_i',k_\perp'^i,\lambda_i')\psi_{+n}^{\uparrow}(x_i,k_\perp^i,\lambda_i)+\psi_{-n}^{\downarrow *}(x_i',k_\perp'^i,\lambda_i')\psi_{+n}^{\downarrow}(x_i,k_\perp^i,\lambda_i)\right][\delta_{\lambda_i',\lambda_i}(i=2\ldots n)]. \tag{21}$$

III. CHIRAL-ODD GPDS OF THE SEA QUARKS

In this section, we present calculations of the chiral-odd GPDs for the $\bar{u}$ and $\bar{d}$ quarks within the proton at zero skewness using the light-cone quark model. The light-cone formalism has been widely applied for computing the PDFs of nucleons and mesons [74]. Within this approach, the wave functions for a hadronic composite state can be expressed as LCWFs in Fock-state basis. Additionally, the overlap representation has been used to study various form factors of the nucleon [13] and the pion [75], the nucleon anomalous magnetic moment [13], as well as GPDs [73]. Here we extend light-cone formalism to calculate the chiral-odd GPDs of the sea quarks.

In the light-cone approach, the wave functions of the hadron describing a composite state at a particular light-cone time are expanded in terms of LCWFs in the Fock-state basis. In order to generate the sea quark degrees of freedom, we employ the baryon-meson fluctuation model [69,76], in which the proton can fluctuate into a composite system consisting of a meson M and a baryon B, where the meson is composed of $q\bar{q}$,

$$|p\rangle \to |MB\rangle \to |q\bar{q}B\rangle. \tag{22}$$

This model has been previously applied to calculate the chiral-even GPDs [76] as well as the collinear PDFs [77] of the nucleon [78] improved by the virtual pion cloud. Here, our focus is specifically on the $\bar{u}$ and $\bar{d}$ quarks.

The LCWFs incorporating sea quark components derived from the model in Ref. [69] take the form [70]

$$\psi^{\lambda_N}_{\lambda_B\lambda_q\lambda_{\bar{q}}}(x,y,\boldsymbol{k}_T,\boldsymbol{r}_T) = \psi^{\lambda_N}_{\lambda_B}(y,\boldsymbol{r}_T)\psi_{\lambda_q\lambda_{\bar{q}}}(x,y,\boldsymbol{k}_T,\boldsymbol{r}_T), \tag{23}$$

where $\psi^{\lambda_N}_{\lambda_B}(y,r_T)$ can be viewed as the wave function of the nucleon in terms of the πB components, and $\psi_{\lambda_q\lambda_{\bar{q}}}(x,y,\boldsymbol{k}_T,\boldsymbol{r}_T)$ is the wave function of the pion in terms of the $q\bar{q}$ components. Here, x and y represent the light-cone momentum fractions, while $\boldsymbol{k}_T$ and $\boldsymbol{r}_T$ denote the transverse momenta of the antiquark and the meson.

For $\psi^{\lambda_N}_{\lambda_B}(y,r_T)$ in Eq. (23), they have the expressions

$$\begin{aligned}
\psi_+^+(y,\boldsymbol{r}_T) &= \frac{M_B-(1-y)M}{\sqrt{1-y}}\phi_1,\\
\psi_-^+(y,\boldsymbol{r}_T) &= \frac{r_1+ir_2}{\sqrt{1-y}}\phi_1,\\
\psi_+^-(y,\boldsymbol{r}_T) &= \frac{r_1-ir_2}{\sqrt{1-y}}\phi_1,\\
\psi_-^-(y,\boldsymbol{r}_T) &= \frac{(1-y)M-M_B}{\sqrt{1-y}}\phi_1.
\end{aligned} \tag{24}$$

Here, M and M_B are the masses of proton and baryon, respectively. ϕ_1 is the wave function of the baryon-meson system in the momentum space with the form

$$\phi_1(y, \boldsymbol{r}_T) = -\frac{g(r^2)\sqrt{y(1-y)}}{\boldsymbol{r}_T^2 + L_1^2(m_\pi^2)}, \tag{25}$$

where m_π is the mass of π meson, $g(r^2)$ is the form factor for the coupling of the nucleon-pion meson-baryon vertex, and

$$L_1^2(m_\pi^2) = yM_B^2 + (1-y)m_\pi^2 - y(1-y)M^2. \tag{26}$$

The pion LCWFs in Eq. (23) have the following expressions:

$$\begin{aligned}
\psi_{++}(x, y, \boldsymbol{k}_T, \boldsymbol{r}_T) &= \frac{my}{\sqrt{x(y-x)}}\phi_2, \\
\psi_{+-}(x, y, \boldsymbol{k}_T, \boldsymbol{r}_T) &= \frac{y(k_1 - ik_2) - x(r_1 - ir_2)}{\sqrt{x(y-x)}}\phi_2, \\
\psi_{-+}(x, y, \boldsymbol{k}_T, \boldsymbol{r}_T) &= \frac{y(k_1 + ik_2) - x(r_1 + ir_2)}{\sqrt{x(y-x)}}\phi_2, \\
\psi_{--}(x, y, \boldsymbol{k}_T, \boldsymbol{r}_T) &= \frac{-my}{\sqrt{x(y-x)}}\phi_2,
\end{aligned} \tag{27}$$

where m is the mass of quarks and sea quarks, and

$$\phi_2(x, y, \boldsymbol{k}_T, \boldsymbol{r}_T) = -\frac{g(k^2)\sqrt{\frac{x}{y}(1-\frac{x}{y})}}{(\boldsymbol{k}_T - \frac{x}{y}\boldsymbol{r}_T)^2 + L_2^2(m^2)} \tag{28}$$

is the wave function of the pion meson in momentum space, with

$$L_2^2(m^2) = \frac{x}{y}m^2 + \left(1 - \frac{x}{y}\right)m^2 - \frac{x}{y}\left(1 - \frac{x}{y}\right)m_\pi{}^2. \tag{29}$$

Here, $g(r^2)$ and $g(k^2)$ are the form factors for the coupling of the nucleon-pion and pion-quark-antiquark vertex, respectively, adopting a the dipolar form

$$g(r^2) = -g_1(1-y)\frac{\boldsymbol{r}_T^2 + L_1^2(m_\pi^2)}{[\boldsymbol{r}_T^2 + L_1^2(\Lambda_\pi^2)]^2}, \tag{30}$$

$$g(k^2) = -g_2\left(1 - \frac{x}{y}\right)\frac{(\boldsymbol{k}_T - \frac{x}{y}\boldsymbol{r}_T)^2 + L_2^2(m^2)}{[(\boldsymbol{k}_T - \frac{x}{y}\boldsymbol{r}_T)^2 + L_2^2(\Lambda_{\bar{q}}^2)]^2}. \tag{31}$$

Using the overlap representation in Eqs. (18)–(21), the chiral-odd GPDs for sea quarks can be calculated from

$$\frac{i\Delta_1\Delta_2}{M^2}\tilde{H}_T = -\sum_{\lambda_B\lambda_q}\int\frac{d^2\boldsymbol{k}_T}{16\pi^3}\int\frac{d^2\boldsymbol{r}_T}{16\pi^3}\left[\psi^{\uparrow *}_{\lambda_B\lambda_q+}(x, y, \boldsymbol{k}'_T, \boldsymbol{r}'_T)\psi^{\downarrow}_{\lambda_B\lambda_q-}(x, y, \boldsymbol{k}_T, \boldsymbol{r}_T) - \psi^{\downarrow *}_{\lambda_B\lambda_q-}(x, y, \boldsymbol{k}'_T, \boldsymbol{r}'_T)\psi^{\uparrow}_{\lambda_B\lambda_q+}(x, y, \boldsymbol{k}_T, \boldsymbol{r}_T)\right], \tag{32}$$

$$2H_T + \frac{\Delta_T^2}{2M^2}\tilde{H}_T = -\sum_{\lambda_B\lambda_q}\int\frac{d^2\boldsymbol{k}_T}{16\pi^3}\int\frac{d^2\boldsymbol{r}_T}{16\pi^3}\left[\psi^{\downarrow *}_{\lambda_B\lambda_q+}(x, y, \boldsymbol{k}'_T, \boldsymbol{r}'_T)\psi^{\uparrow}_{\lambda_B\lambda_q-}(x, y, \boldsymbol{k}_T, \boldsymbol{r}_T) + \psi^{\uparrow *}_{\lambda_B\lambda_q-}(x, y, \boldsymbol{k}'_T, \boldsymbol{r}'_T)\psi^{\downarrow}_{\lambda_B\lambda_q+}(x, y, \boldsymbol{k}_T, \boldsymbol{r}_T)\right], \tag{33}$$

$$\frac{\Delta_1 + i\Delta_2}{2M}\tilde{E}_T = -\sum_{\lambda_B\lambda_q}\int\frac{d^2\boldsymbol{k}_T}{16\pi^3}\int\frac{d^2\boldsymbol{r}_T}{16\pi^3}\left[\psi^{\uparrow *}_{\lambda_B\lambda_q-}(x, y, \boldsymbol{k}'_T, \boldsymbol{r}'_T)\psi^{\uparrow}_{\lambda_B\lambda_q+}(x, y, \boldsymbol{k}_T, \boldsymbol{r}_T) - \psi^{\downarrow *}_{\lambda_B\lambda_q-}(x, y, \boldsymbol{k}'_T, \boldsymbol{r}'_T)\psi^{\downarrow}_{\lambda_B\lambda_q+}(x, y, \boldsymbol{k}_T, \boldsymbol{r}_T)\right], \tag{34}$$

$$\begin{aligned}
\frac{\Delta_1 + i\Delta_2}{2M}(2\tilde{H}_T + E_T) = -\sum_{\lambda_B\lambda_q}\int\frac{d^2\boldsymbol{k}_T}{16\pi^3}\int\frac{d^2\boldsymbol{r}_T}{16\pi^3}\Big[&\psi^{\uparrow *}_{\lambda_B\lambda_q-}(x, y, \boldsymbol{k}'_T, \boldsymbol{r}'_T)\psi^{\uparrow}_{\lambda_B\lambda_q+}(x, y, \boldsymbol{k}_T, \boldsymbol{r}_T) \\
&+ \psi^{\downarrow *}_{\lambda_B\lambda_q-}(x, y, \boldsymbol{k}'_T, \boldsymbol{r}'_T)\psi^{\downarrow}_{\lambda_B\lambda_q+}(x, y, \boldsymbol{k}_T, \boldsymbol{r}_T)\Big],
\end{aligned} \tag{35}$$

where

$$\begin{aligned}
\boldsymbol{k}''_T &= \boldsymbol{k}_T - \frac{1}{2}(1-x)\boldsymbol{\Delta}_T, \\
\boldsymbol{k}'_T &= \boldsymbol{k}_T + \frac{1}{2}(1-x)\boldsymbol{\Delta}_T
\end{aligned} \tag{36}$$

are the transverse momenta for the final- and initial-state struck antiquarks,

$$
\begin{aligned}
-\boldsymbol{r}_T'' &= -\boldsymbol{r}_T + \frac{1}{2}(1-y)\boldsymbol{\Delta}_T, \\
-\boldsymbol{r}_T' &= -\boldsymbol{r}_T - \frac{1}{2}(1-y)\boldsymbol{\Delta}_T, \\
(\boldsymbol{r}_T - \boldsymbol{k}_T)'' &= (\boldsymbol{r}_T - \boldsymbol{k}_T) + \frac{1}{2}(y-x)\boldsymbol{\Delta}_T, \\
(\boldsymbol{r}_T - \boldsymbol{k}_T)' &= (\boldsymbol{r}_T - \boldsymbol{k}_T) - \frac{1}{2}(y-x)\boldsymbol{\Delta}_T
\end{aligned} \tag{37}
$$

are the transverse momenta for the final and initial spectators B and q, respectively.

Substituting the light-cone wave functions of the proton in Eqs. (24) and (27), we obtain the expressions for the chiral-odd GPDs of the sea quarks as follows:

$$\tilde{E}_T^{\bar{q}/P}(x,0,t) = 0, \tag{38}$$

$$H_T^{\bar{q}/P}(x,0,t) = 0, \tag{39}$$

$$\tilde{H}_T^{\bar{q}/P}(x,0,t) = \frac{g_1^2 g_2^2}{(2\pi)^6}\int_x^1 \frac{dy}{y}\int d^2\boldsymbol{k}_T \int d^2\boldsymbol{r}_T \frac{y(1-y)^3(1-\frac{x}{y})^3 M^2 m[M_B-(1-y)M]}{D_1(y,\boldsymbol{r}_T,\boldsymbol{\Delta}_T)D_2(\frac{x}{y},\boldsymbol{k}_T-\frac{x}{y}\boldsymbol{r}_T,\boldsymbol{\Delta}_T)}, \tag{40}$$

$$E_T^{\bar{q}/P}(x,0,t) = \frac{g_1^2 g_2^2}{(2\pi)^6}\int_x^1 \frac{dy}{y}\int d^2\boldsymbol{k}_T \int d^2\boldsymbol{r}_T \tag{41}$$

$$\frac{y(1-y)^2(1-\frac{x}{y})^3\{Mm[[M_B-(1-y)M]^2+\boldsymbol{r}_T^2-\frac{1}{4}(1-y)\boldsymbol{\Delta}_T^2]-2M^2m(1-y)[M_B-(1-y)M]\}}{D_1(y,\boldsymbol{r}_T,\boldsymbol{\Delta}_T)D_2(\frac{x}{y},\boldsymbol{k}_T-\frac{x}{y}\boldsymbol{r}_T,\boldsymbol{\Delta}_T)}, \tag{42}$$

where

$$D_1(y,\boldsymbol{r}_T,\boldsymbol{\Delta}_T) = \left[\left(\boldsymbol{r}_T - \frac{1}{2}(1-y)\boldsymbol{\Delta}_T\right)^2 + L_1^2\right]^2\left[(\mathbf{r}_T + \frac{1}{2}(1-y)\boldsymbol{\Delta}_T)^2 + L_1^2\right]^2, \tag{43}$$

$$D_2\left(\frac{x}{y},\boldsymbol{k}_T-\frac{x}{y}\boldsymbol{r}_T,\boldsymbol{\Delta}_T\right) = \left[\left[\left(\boldsymbol{k}_T-\frac{x}{y}\boldsymbol{r}_T\right)-\frac{1}{2}\left(1-\frac{x}{y}\right)\boldsymbol{\Delta}_T\right]^2+L_2^2\right]^2\left[\left[\left(\boldsymbol{k}_T-\frac{x}{y}\boldsymbol{r}_T\right)+\frac{1}{2}\left(1-\frac{x}{y}\right)\boldsymbol{\Delta}_T\right]^2+L_2^2\right]^2. \tag{44}$$

Our results show that two chiral-odd GPDs of the antiquarks $\tilde{E}_T^{\bar{q}/P}(x,\xi,t)$ and $H_T^{\bar{q}/P}(x,\xi,t)$ vanish at zero skewness.

$\tilde{E}_T$ does not contribute at $\xi = 0$ because it is an odd function of ξ, consistent with our model calculation result. As for H_T, it reduces to the transversity distribution h_1 in the forward limit,

$$H_T^{\bar{q}/P}(x,0,0) = h_1^{\bar{q}/P}(x). \tag{45}$$

$h_1^{\bar{u}/P}$ and $h_1^{\bar{d}/P}$ are zero in our model. The sea quark transversity distributions are usually assumed to be zero in many analyses due to the fact that quark transversity distributions do not mix with gluons in the evolution. In a recent phenomenological extraction of transversity distribution functions by simultaneously fitting to semi-inclusive deep inelastic scattering and e^+e^- annihilation data [79], it was found that the $\bar{u}$ quark favors a negative transversity distribution while that of the $\bar{d}$ quark is consistent with zero with current accuracy. In Ref. [77], the calculations of the antiquark transversity distributions within the meson-cloud approach were presented for the first time, showing both the up antiquark and the down antiquark have negative results, albeit very small.

The differences in these results may arise because our model calculation includes $\bar{u}$ and $\bar{d}$ flavors in one expression, providing less constraint. The chiral-odd GPD H_T can be constrained from independent measurements on the transverse distribution $h_1(x)$ and the tensor charge $\delta q = \int dx h_1(x)$, which can be evaluated from the integral of the transversity distribution. Since h_1 is the observable that we aim to determine from GPDs, the constraint in the forward limit is not quantitatively useful but just serves as an indication [44]. The chiral-odd GPD H_T with the forward limit constraint imposed can be fitted by

TABLE I. Values of the parameters taken from Ref. [70].

Parameters	$\bar{u}$	$\bar{d}$
g_1	9.33	5.79
g_2	4.46	4.46
Λ_π (GeV)	0.223	0.223
$\Lambda_{\bar{q}}$ (GeV)	0.510	0.510

comparing it with the experimentally extracted h_1. However, in our calculation $H_T^{\bar{q}/P} = 0$, which is a model-dependent result and means that our result on $H_T^{\bar{q}/P}$ is less constrained.

IV. NUMERICAL RESULTS FOR CHIRAL-ODD GPDS OF SEA QUARKS

In this section, we present the numerical results for the chiral-odd GPDs of the sea quarks in momentum as well as impact parameter space. To do this, we need to specify the values of the parameters in our model. We choose the values from Ref. [70], shown in Table I.

As shown in Ref. [70], the values of g_2 and Λ_π are fixed by adopting the Gluck-Reya-Vogt leading-order (LO) parametrizations [80] to perform the fit for $f_1^{\bar{u}/\pi^-}$ [or $f_1^{\bar{d}/\pi^+}(x)$]. The Martin-Stirling-Thorne-Watt 2008 LO parametrization [81] is adopted for $f_1^{\bar{u}/P}$ and $f_1^{\bar{d}/P}$ to obtain the values of the parameters g_1 and $\Lambda_{\bar{q}}$.

Using parameter values from Table I, we numerically calculate the sea quark chiral-odd GPDs at the model scale. In the left and right panels of Fig. 1, we depict the $\tilde{H}_T^{\bar{q}/P}(x, 0, -\boldsymbol{\Delta}_T^2)$ (multiplied by a prefactor x) of $\bar{u}$ and $\bar{d}$ quarks as functions of the momentum fraction x and the momentum transfer Δ_T, respectively. We observe that $x\tilde{H}_T^{\bar{q}/P}(x, 0, -\boldsymbol{\Delta}_T^2)$ is substantial, peaking around $x = 0.08$, with a maximum magnitude of 0.4. In both cases of $\bar{u}$ and $\bar{d}$, $x\tilde{H}_T^{\bar{u}/P}$ and $x\tilde{H}_T^{\bar{d}/P}$ are positive in the entire x and Δ_T region. The peak of the curves shifts toward smaller x region as Δ_T decreases.

In Fig. 2, $xE_T^{\bar{q}/P}(x, 0, -\boldsymbol{\Delta}_T^2)$ of the $\bar{u}$ and $\bar{d}$ quarks is plotted as a function of x and Δ_T. The magnitude of $xE_T^{\bar{q}/P}(x, 0, -\boldsymbol{\Delta}_T^2)$ is similar to that of $x\tilde{H}_T^{\bar{q}/P}(x, 0, -\boldsymbol{\Delta}_T^2)$, but its sign is negative. Similar to $x\tilde{H}_T^{\bar{q}/P}$, $xE_T^{\bar{u}/P}$, and $xE_T^{\bar{d}/P}$ peak at lower x ($0 < x < 0.1$). For a fixed Δ_T value, $xE_T^{\bar{u}/P}$ and $xE_T^{\bar{d}/P}$ decrease monotonically with increasing Δ_T.

Next, we examine the chiral-odd GPDs in transverse position space. The GPDs in transverse position space are defined by introducing the Fourier conjugate $\boldsymbol{b}_T$ (impact parameter) of the transverse momentum transfer Δ_T as follows [23]:

$$\mathcal{H}_T(x, 0, \boldsymbol{b}_T) = \int \frac{d^2\boldsymbol{\Delta}_T}{(2\pi)^2} e^{-i\boldsymbol{\Delta}_T\cdot\boldsymbol{b}_T} H_T(x, 0, t), \quad (46)$$

$$\mathcal{E}_T(x, 0, \boldsymbol{b}_T) = \int \frac{d^2\boldsymbol{\Delta}_T}{(2\pi)^2} e^{-i\boldsymbol{\Delta}_T\cdot\boldsymbol{b}_T} E_T(x, 0, t), \quad (47)$$

$$\tilde{\mathcal{H}}_T(x, 0, \boldsymbol{b}_T) = \int \frac{d^2\boldsymbol{\Delta}_T}{(2\pi)^2} e^{-i\boldsymbol{\Delta}_T\cdot\boldsymbol{b}_T} \tilde{H}_T(x, 0, t). \quad (48)$$

Here, $\boldsymbol{b}_T$ denotes a measure of the transverse distance between the struck parton and the center of momentum of the hadron. In our study, we set $\xi = 0$, which means that the momentum transfer occurs entirely in the transverse direction. In the Dokshitzer-Gribov-Lipatov-Altarelli-Parisi region $\xi < x < 1$ [82], the impact parameter b_T provides the transverse location of the parton where it is pulled out and put back to the nucleon, as well as the relative distance between the struck parton and the spectators.

In Figs. 3 and 4, we present the numerical results of the chiral-odd GPDs of sea quarks in impact parameter space as functions of x and b_T. We observe that $x\tilde{\mathcal{H}}_T^{\bar{q}/P}$ and $x\mathcal{E}_T^{\bar{q}/P}$ for $\bar{u}$ and $\bar{d}$ quarks peak at $b_T = 0$. To be specific, for any given x, the peak of these curves decrease with increasing b_T. Moreover, we find that the position of the peak is located at similar x region for any given b_T. In addition, $x\tilde{\mathcal{H}}_T^{\bar{u}/P}$ and $x\tilde{\mathcal{H}}_T^{\bar{d}/P}$ are positive, while $x\mathcal{E}_T^{\bar{u}/P}$ and $x\mathcal{E}_T^{\bar{d}/P}$ are negative in the entire x and b_T region. For any given x and b_T, the chiral-odd GPDs in impact parameter space of the $\bar{d}$ quark is larger than that of the $\bar{u}$ quark.

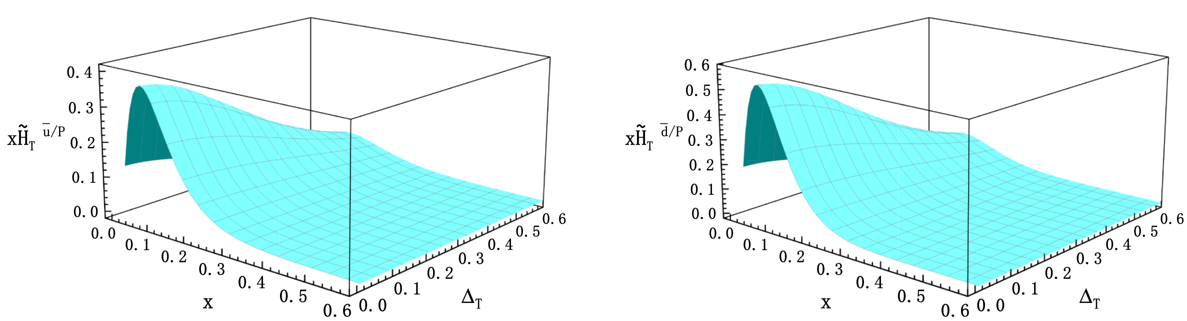

FIG. 1. The chiral-odd GPDs in momentum space $\tilde{H}_T^{\bar{u}/P}(x, 0, -\boldsymbol{\Delta}_T^2)$ and $\tilde{H}_T^{\bar{d}/P}(x, 0, -\boldsymbol{\Delta}_T^2)$ in the light-cone quark model as functions of x and Δ_T.

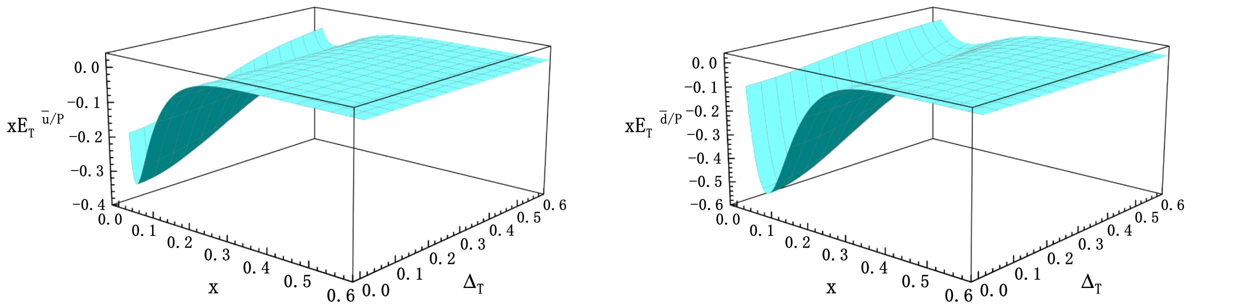

FIG. 2. The chiral-odd GPDs in momentum space $E_T^{\bar{u}/P}(x,0,-\boldsymbol{\Delta}_T^2)$ and $E_T^{\bar{d}/P}(x,0,-\boldsymbol{\Delta}_T^2)$ in the light-cone quark model as functions of x and Δ_T.

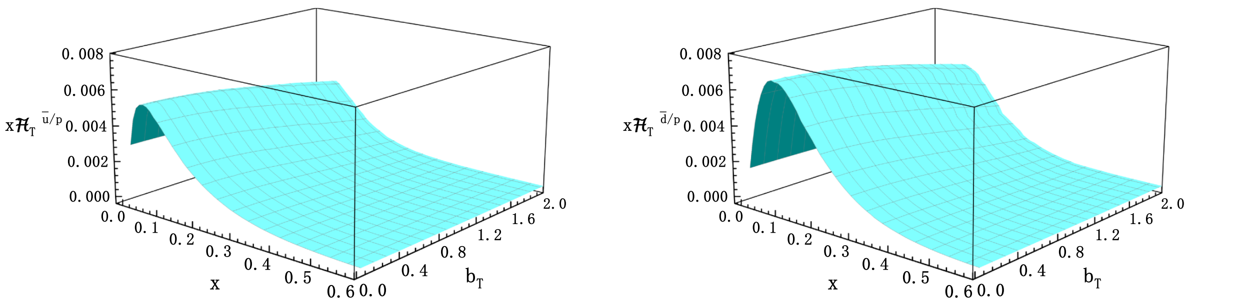

FIG. 3. The chiral-odd GPDs in the impact parameter space $\tilde{\mathcal{H}}_T^{\bar{u}/P}(x,0,\boldsymbol{b}_T)$ and $\tilde{\mathcal{H}}_T^{\bar{d}/P}(x,0,\boldsymbol{b}_T)$ in the light-cone quark model as functions of x and b_T.

Similar to the chiral-even GPDs, the chiral-odd GPDs also have an interesting interpretation in impact parameter space. At $\xi = 0$, the chiral-odd GPDs can be interpreted in terms of parton density, depending on the polarization of both the active quark and the nucleon [58]. Moreover, specific combinations of the chiral-odd GPDs in impact parameter space affect the quark and nucleon spin correlations in different ways [20]. For example, the combination $H_T + \frac{\Delta_T^2}{4M^2}\tilde{H}_T$ reduces to the transversity distribution $h_1(x)$ in the forward limit. The corresponding distribution in the impact parameter space $\mathcal{H}_T - \frac{\Delta_b}{4m^2}\tilde{\mathcal{H}}_T$ relates to the correlation between the transverse spin of the quark and the spin of transversely polarized proton [20], where $\Delta_b f$ is defined as

$$\Delta_b f = \frac{\partial}{\partial b^i}\frac{\partial}{\partial b^i} f = 4\frac{\partial}{\partial b^2}\left(b^2\frac{\partial}{\partial b^2}\right) f. \tag{49}$$

Similarly, $E_T + 2\tilde{H}_T$ describes the transverse deformation in the center-of-momentum frame due to spin-orbit correlations. In the impact parameter space, $\mathcal{E}_T + 2\tilde{\mathcal{H}}_T$ represents a sideways shift in the distribution of transversely polarized quarks in an unpolarized proton. Furthermore, $E_T + 2\tilde{H}_T$ is related to the Boer-Mulders function, and its first moment can be interpreted as the transverse anomalous magnetic moment of the proton κ_T [21,83]. Finally, the combination $\epsilon_{ij} b_j \frac{\partial}{\partial B}(\mathcal{E}_T + 2\tilde{\mathcal{H}}_T)$ reflects the spin-orbit correlation of quarks within the proton, contributing to the spin density.

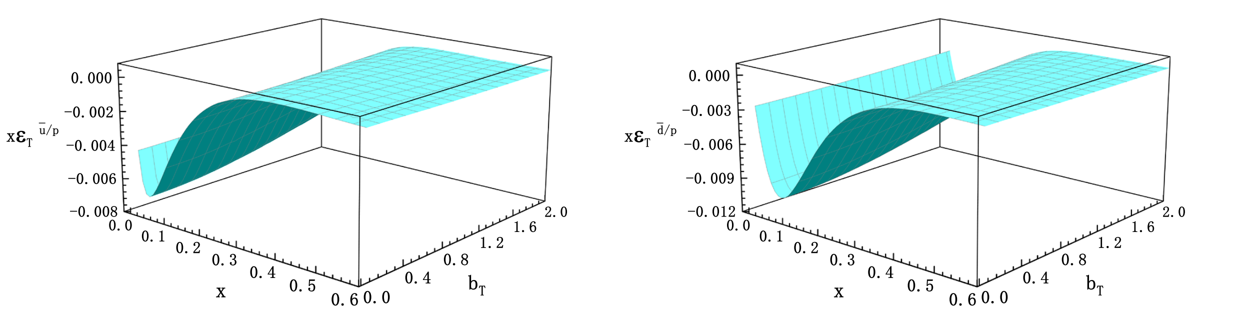

FIG. 4. The chiral-odd GPDs in impact parameter space $\mathcal{E}_T^{\bar{u}/P}(x,0,\boldsymbol{b}_T)$ and $\mathcal{E}_T^{\bar{d}/P}(x,0,\boldsymbol{b}_T)$ in the light-cone quark model as functions of x and b_T.

Here we write these combinations in the $\boldsymbol{b}_T$ space as [60]

$$f_T(x,0,\boldsymbol{b}_T) = \mathcal{H}_T(x,0,\boldsymbol{b}_T) - \frac{\Delta_b}{4M^2}\tilde{\mathcal{H}}_T(x,0,\boldsymbol{b}_T)$$
$$= \int \frac{d^2\boldsymbol{\Delta}_T}{(2\pi)^2} e^{-i\boldsymbol{\Delta}_T\cdot\boldsymbol{b}_T}\left[H_T(x,0,t) + \frac{\Delta_T^2}{4M^2}\tilde{H}_T(x,0,t)\right], \tag{50}$$

$$F_T(x,0,\boldsymbol{b}_T) = \mathcal{E}_T(x,0,\boldsymbol{b}_T) + 2\tilde{\mathcal{H}}_T(x,0,\boldsymbol{b}_T)$$
$$= \int \frac{d^2\boldsymbol{\Delta}_T}{(2\pi)^2} e^{-i\boldsymbol{\Delta}_T\cdot\boldsymbol{b}_T}\left[E_T(x,0,t) + 2\tilde{H}_T(x,0,t)\right], \tag{51}$$

and the spin-orbit correlation

$$F_T^i(x,0,\boldsymbol{b}_T) = -\epsilon^{ij}b_j\frac{\partial}{\partial B}\left[\mathcal{E}_T(x,0,\boldsymbol{b}_T) + 2\tilde{\mathcal{H}}_T(x,0,\boldsymbol{b}_T)\right]$$
$$= i\epsilon^{ij}\int \frac{d^2\boldsymbol{\Delta}_T}{(2\pi)^2}\Delta_j e^{-i\boldsymbol{\Delta}_T\cdot\boldsymbol{b}_T}\left[E_T(x,0,t) + 2\tilde{H}_T(x,0,t)\right]$$
$$= -i\frac{\epsilon^{ij}b_j}{b}\int\frac{(\Delta)^2 d\Delta}{2\pi}\left[E_T(x,0,t) + 2\tilde{H}_T(x,0,t)\right]J_1(b\Delta), \tag{52}$$

where

$$\frac{\partial}{\partial B} = 2\frac{\partial}{\partial b^2}, \qquad b_1 = b_T\cos\phi, \qquad b_2 = b_T\sin\phi, \tag{53}$$

and

$$J_n(b\Delta) = \frac{1}{\pi}\int_0^\pi d\theta\,\cos(n\theta - b\Delta\sin\theta). \tag{54}$$

In Fig. 5, we depict the x dependence of $f_T(x,0,\boldsymbol{b}_T)$ for the $\bar{u}$ (left figure) and $\bar{d}$ (right figure) quarks at fixed impact parameter $b_T = 0.5$, 1.0, and 2.0 GeV^{-1}, respectively. We find that $xf_T(x,0,\boldsymbol{b}_T)$ of the $\bar{u}$ and $\bar{d}$ quarks exhibit positive tendency, and the large contribution is concentrated in the region $x < 0.4$. As b_T increases, the magnitude of $xf_T(x,0,\boldsymbol{b}_T)$ decreases, shifting the peak of the curve toward smaller x region.

In Fig. 6, we present $xF_T(x,0,\boldsymbol{b}_T)$ as a function of x at different values of b_T. Here, $xF_T^{\bar{u}/P}$ and $xF_T^{\bar{d}/P}$ remain

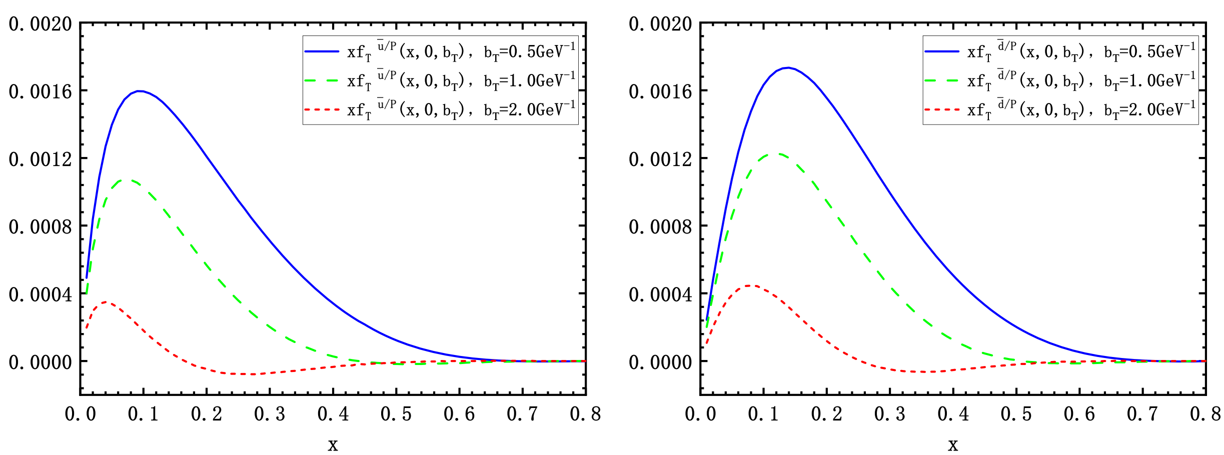

FIG. 5. $xf_T^{\bar{u}/P}(x,0,\boldsymbol{b}_T)$ and $xf_T^{\bar{d}/P}(x,0,\boldsymbol{b}_T)$ in the light-cone quark model as a function of x at $b_T = 0.5$, 1.0, and 2.0 GeV^{-1}.

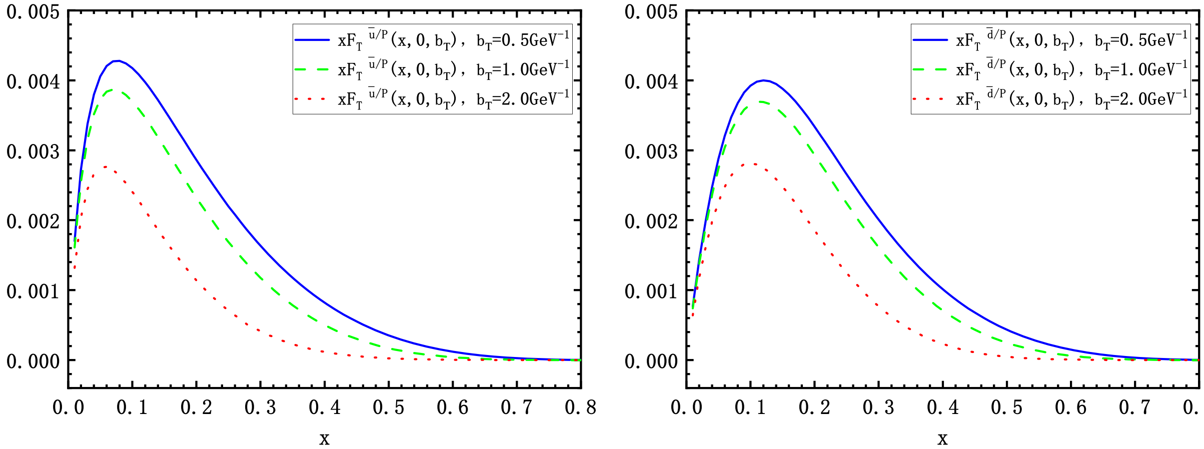

FIG. 6. $xF_T^{\bar{u}/P}(x, 0, \boldsymbol{b}_T)$ and $xF_T^{\bar{d}/P}(x, 0, \boldsymbol{b}_T)$ in the light-cone quark model as a function of x at $b_T = 0.5$, 1.0, and 2.0 GeV^{-1}.

positive and decrease in magnitude with increasing b_T, similar to behavior observed in $xf_T(x, 0, \boldsymbol{b}_T)$. Another observation is that the sizes and shapes of $xF_T^{\bar{u}/P}$ and $xF_T^{\bar{d}/P}$ are quite similar.

Figure 7 displays $xF_T^i(x, 0, \boldsymbol{b}_T)$ as a function of x for different b_T values, where we neglect the constant phase factor (i) and take $\epsilon^{ij} = \epsilon^{12}$. The distributions for both the $\bar{u}$ and $\bar{d}$ quarks are negative. This observation highlights the interplay between quark spin and orbital angular momentum, as described by the term $\epsilon i j b_j \frac{\partial}{\partial B}(\mathcal{E}T + 2\tilde{\mathcal{H}}T)$.

In Fig. 8, we plot $xF_T^i(x, 0, \boldsymbol{b}_T)$ as a function of x at fixed $b_T = 1.0$ GeV^{-1}, varying ϕ values (20°, 30°, and 60°). Among f_T, F_T, and F_T^i, F_T exhibits the largest magnitude, reaching up to 0.004. In contrast, F_T^i is notably smaller compared to F_T.

As there have been no calculations for the chiral-odd GPDs of sea quarks using other models, nor for the chiral-odd GPDs of valence quarks using the baryon-meson fluctuation model so far, we compare our results to those for the valence quark with other model calculations for qualitative and quantitative discussion. Our model calculations show that the chiral-odd GPDs for sea quarks $H_T^{\bar{u}/P}$ and $H_T^{\bar{d}/P}$ are zero. On the contrary, $H_T^{u/P}$ and $H_T^{d/P}$ are nonzero for valence quarks, as shown in Refs. [44,56–58].

In Ref. [57], the chiral-odd GPDs of valence quarks were calculated in the light-front constituent quark model (LFCQM). We observe that the signs of $\tilde{H}_T^{\bar{q}/P}$ and $E_T^{\bar{q}/P}$ in our model differ from those of $\tilde{H}_T^{q/P}$ and $E_T^{q/P}$ in Ref. [57], where $\tilde{H}_T$ or E_T for u and d quarks have opposite signs, while the signs of these GPDs for $\bar{u}$ and $\bar{d}$ quarks are the same in our model. In addition, it is found that the sizes of $\tilde{H}_T^{d/P}$ and $E_T^{u/P}$ can reach to 2.6 and 9.0, respectively, which are larger than the sizes of $\tilde{H}_T^{u/P}$ and $\tilde{H}_T^{d/P}$ (1.7 in maximum) and $E_T^{d/P}$ (1.2 in maximum). In contrast, the magnitude of $E_T^{\bar{d}/P}$ for the $\bar{u}$ quark are smaller than those for the $\bar{d}$ quark in our model.

Furthermore, we find that the x shapes of $\tilde{H}_T^{\bar{q}/P}$ and $E_T^{\bar{q}/P}$ for sea quarks in our model are similar to those of the two chiral-odd GPDs for valence quarks in Ref. [57]. The LFCQM was also employed to calculate the chiral-odd

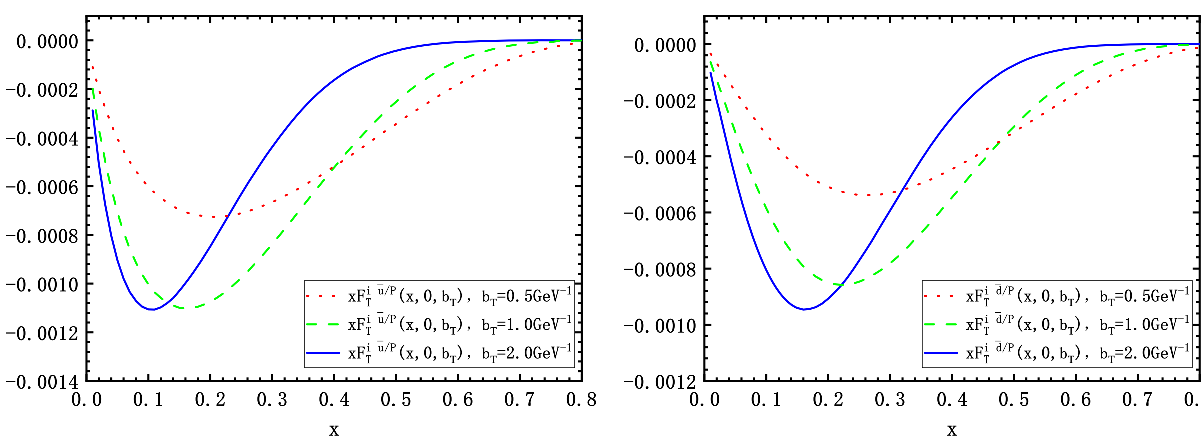

FIG. 7. $xF_T^{i\bar{u}/P}(x, 0, \boldsymbol{b}_T)$ and $xF_T^{i\bar{d}/P}(x, 0, \boldsymbol{b}_T)$ in the light-cone quark model as a function of x at $b_T = 0.5$, 1.0, and 2.0 GeV^{-1}.

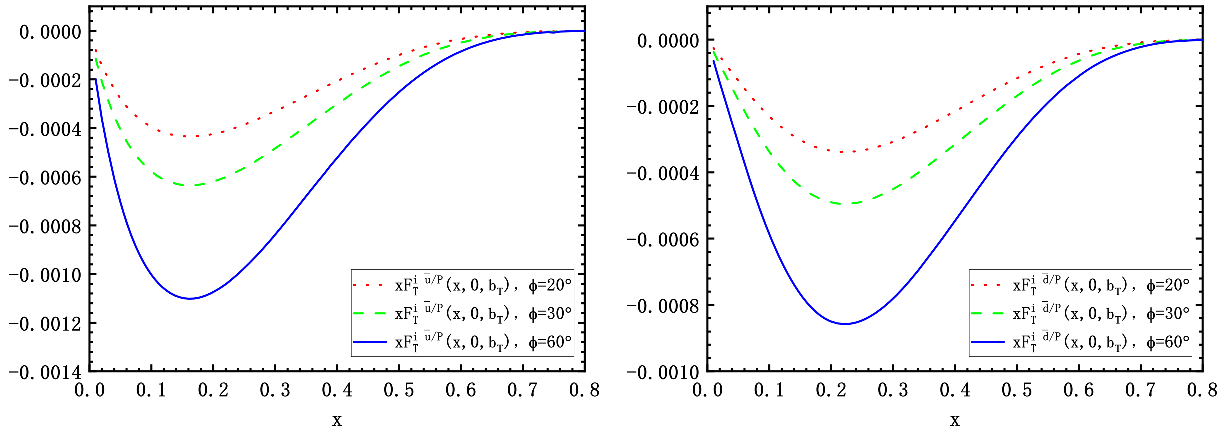

FIG. 8. $xF_T^{i\bar{u}/P}(x,0,\boldsymbol{b}_T)$ and $xF_T^{i\bar{d}/P}(x,0,\boldsymbol{b}_T)$ in the light-cone quark model as a function of x at $\phi = 20°, 30°$, and $60°$.

GPDs for valence quarks in Ref. [56], where opposite signs were found for $\tilde{H}_T$ of the u and d quarks and same signs for $E_T^{u/P}$ and $E_T^{d/P}$. In Ref. [58], the chiral-odd GPDs of valence quarks were calculated using the light-front quark-diquark model, showing agreement in sign and size for $\tilde{H}_T^{q/P}$ or $E_T^{q/P}$ of the u and d quarks as in Ref. [57]. Particularly, the x dependence and Δ_T dependence of these two chiral-odd GPDs are similar to our results for sea quarks.

In Ref. [44], chiral-odd GPDs of u and d quarks were explored using a parametrization based on the Reggeized diquark model. It was found that $E_T^{u/P}$ and $E_T^{d/P}$ are positive, while our results for $E_T^{\bar{u}/P}$ and $E_T^{\bar{d}/P}$ are negative. In this model, $\tilde{H}_T^{u/P}$ is positive and $\tilde{H}_T^{d/P}$ vanishes. As a comparison, $\tilde{H}_T^{\bar{u}/P}$ and $\tilde{H}_T^{\bar{d}/P}$ are both positive in our model. Finally, the chiral-odd GPDs in transverse impact parameter space were also calculated in Ref. [58], which showed a similar b_T dependence compared to our results.

V. CONCLUSION

In this work, we studied the chiral-odd GPDs of the sea quarks within the proton using a light-cone quark model. We utilized the overlap representation to express the chiral-odd GPDs in term of the LCWF of the proton. The sea quark degrees of freedom are generated by considering the Fock states of the proton as a composite system consist of a pion meson and a baryon, where the pion meson is composed in terms of $q\bar{q}$. Using the overlap representation of LCWFs, we obtained the analytic results of the chiral-odd GPDs of sea quarks at $\xi = 0$. It is found that $H_T^{\bar{q}/P}(x,0,-\boldsymbol{\Delta}_T^2)$ vanishes in our model. Numerical calculations for $\tilde{H}_T^{\bar{q}/P}(x,0,-\boldsymbol{\Delta}_T^2)$ and $E_T^{\bar{q}/P}(x,0,-\boldsymbol{\Delta}_T^2)$ are performed for $\bar{q} = \bar{u}$ and $\bar{d}$, showing that these two GPDs are sizable, and $\tilde{H}_T^{\bar{q}/P}(x,0,-\boldsymbol{\Delta}_T^2)$ is positive while $E_T^{\bar{q}/P}(x,0,-\boldsymbol{\Delta}_T^2)$ is negative. We also calculated $\mathcal{H}_T^{\bar{q}/P}(x,0,\boldsymbol{b}_T)$, $\mathcal{E}_T^{\bar{q}/P}(x,0,\boldsymbol{b}_T)$, and $\tilde{\mathcal{H}}_T^{\bar{q}/P}(x,0,\boldsymbol{b}_T)$, which are the distributions in the impact parameter space. The numerical results demonstrate that these distributions decrease with increasing b_T. To quantitatively examine the spin-orbit correlation effect of sea quarks, we evaluated the combinations such as $\mathcal{H}_T - \frac{\Delta_b}{4M^2}\tilde{\mathcal{H}}_T$, $\mathcal{E}_T + 2\tilde{\mathcal{H}}_T$, and $\epsilon_{ij} b_j \frac{\partial}{\partial B}(\mathcal{E}_T + 2\tilde{\mathcal{H}}_T)$. Among them, $\mathcal{E}_T + 2\tilde{\mathcal{H}}_T$, which describes the sideways shift of the transversely polarized quarks in an unpolarized proton, exhibits a maximum size of 0.004, showing that the spin-orbital correlation of the sea quarks may not be neglected. This study may provide valuable insights into the sea quark distribution within the proton in both transverse momentum and impact parameter space.

ACKNOWLEDGMENTS

This work is partially supported by the National Natural Science Foundation of China under Grant No. 12150013.

[1] D. Müller, D. Robaschik, B. Geyer, F. M. Dittes, and J. Hořejši, Fortschr. Phys. **42**, 101 (1994).
[2] X. D. Ji, Phys. Rev. D **55**, 7114 (1997).
[3] A. V. Radyushkin, Phys. Rev. D **56**, 5524 (1997).
[4] M. Diehl, Eur. Phys. J. A **52**, 149 (2016).
[5] A. V. Radyushkin, Phys. Lett. B **380**, 417 (1996).
[6] A. V. Belitsky, D. Mueller, and A. Kirchner, Nucl. Phys. **B629**, 323 (2002).
[7] S. V. Goloskokov and P. Kroll, Eur. Phys. J. C **50**, 829 (2007).

[8] S. V. Goloskokov and P. Kroll, Eur. Phys. J. C **53**, 367 (2008).
[9] S. V. Goloskokov and P. Kroll, Eur. Phys. J. C **65**, 137 (2010).
[10] S. V. Goloskokov and P. Kroll, Eur. Phys. J. A **47**, 112 (2011).
[11] L. M. Sehgal, Phys. Rev. D **10**, 1663 (1974); **11**, 2016(E) (1975).
[12] P. Kroll, Mod. Phys. Lett. A **35**, 2050093 (2020).
[13] S. J. Brodsky, D. S. Hwang, B. Q. Ma, and I. Schmidt, Nucl. Phys. **B593**, 311 (2001).
[14] N. Kumar and H. Dahiya, Mod. Phys. Lett. A **29**, 1450118 (2014).
[15] G. A. Miller, Annu. Rev. Nucl. Part. Sci. **60**, 1 (2010).
[16] N. Kumar and H. Dahiya, Phys. Rev. D **90**, 094030 (2014).
[17] H. Hashamipour, M. Goharipour, K. Azizi, and S. V. Goloskokov, Phys. Rev. D **105**, 054002 (2022).
[18] H. Hashamipour, M. Goharipour, K. Azizi, and S. V. Goloskokov, Phys. Rev. D **107**, 096005 (2023).
[19] F. Irani, M. Goharipour, H. Hashamipour, and K. Azizi, Phys. Rev. D **108**, 074018 (2023).
[20] M. Diehl and P. Hagler, Eur. Phys. J. C **44**, 87 (2005).
[21] M. Burkardt, Phys. Rev. D **72**, 094020 (2005).
[22] R. D. Pisarski, Phys. Rev. D **62**, 111501 (2000).
[23] M. Burkardt, Int. J. Mod. Phys. A **18**, 173 (2003).
[24] C. Adloff *et al.* (H1 Collaboration), Eur. Phys. J. C **13**, 371 (2000).
[25] C. Adloff *et al.* (H1 Collaboration), Phys. Lett. B **517**, 47 (2001).
[26] A. Aktas *et al.* (H1 Collaboration), Eur. Phys. J. C **44**, 1 (2005).
[27] J. Breitweg *et al.* (ZEUS Collaboration), Eur. Phys. J. C **6**, 603 (1999).
[28] S. Chekanov *et al.* (ZEUS Collaboration), Phys. Lett. B **573**, 46 (2003).
[29] A. Airapetian *et al.* (HERMES Collaboration), Phys. Rev. Lett. **87**, 182001 (2001).
[30] A. Airapetian *et al.* (HERMES Collaboration), Phys. Lett. B **704**, 15 (2011).
[31] A. Airapetian *et al.* (HERMES Collaboration), J. High Energy Phys. 07 (2012) 032.
[32] N. d'Hose, E. Burtin, P. A. M. Guichon, and J. Marroncle, Eur. Phys. J. A **19S1**, 47 (2004).
[33] S. Stepanyan *et al.* (CLAS Collaboration), Phys. Rev. Lett. **87**, 182002 (2001).
[34] M. V. Polyakov, Nucl. Phys. **B555**, 231 (1999).
[35] J. C. Collins, L. Frankfurt, and M. Strikman, Phys. Rev. D **56**, 2982 (1997).
[36] S. Ahmad, G. R. Goldstein, and S. Liuti, Phys. Rev. D **79**, 054014 (2009).
[37] G. R. Goldstein, J. O. Hernandez, and S. Liuti, Phys. Rev. D **84**, 034007 (2011).
[38] R. Boussarie, B. Pire, L. Szymanowski, and S. Wallon, J. High Energy Phys. 02 (2017) 054; 10 (2018) 029.
[39] D. Y. Ivanov, B. Pire, L. Szymanowski, and O. V. Teryaev, Phys. Lett. B **550**, 65 (2002).
[40] R. Enberg, B. Pire, and L. Szymanowski, Eur. Phys. J. C **47**, 87 (2006).
[41] W. Cosyn, B. Pire, and L. Szymanowski, Phys. Rev. D **102**, 054003 (2020).
[42] C. Adolph *et al.* (COMPASS Collaboration), Phys. Lett. B **731**, 19 (2014).
[43] S. V. Goloskokov and P. Kroll, Eur. Phys. J. C **74**, 2725 (2014).
[44] G. R. Goldstein, J. O. Gonzalez Hernandez, and S. Liuti, Phys. Rev. D **91**, 114013 (2015).
[45] M. Diehl and W. Kugler, Eur. Phys. J. C **52**, 933 (2007).
[46] G. Duplančić, D. Müller, and K. Passek-Kumerički, Phys. Lett. B **771**, 603 (2017).
[47] M. Siddikov and I. Schmidt, Phys. Rev. D **99**, 116005 (2019).
[48] I. Bedlinskiy *et al.* (CLAS Collaboration), Phys. Rev. C **90**, 025205 (2014).
[49] I. Bedlinskiy *et al.* (CLAS Collaboration), Phys. Rev. C **95**, 035202 (2017).
[50] A. Kim, H. Avakian, V. Burkert, K. Joo, W. Kim, K. P. Adhikari, Z. Akbar, S. Anefalos Pereira, R. A. Badui, M. Battaglieri *et al.*, Phys. Lett. B **768**, 168 (2017).
[51] B. Zhao *et al.* (CLAS Collaboration), Phys. Lett. B **789**, 426 (2019).
[52] M. E. Beiyad, B. Pire, M. Segond, L. Szymanowski, and S. Wallon, Proc. Sci. DIS2010 (**2010**) 252 [arXiv:1006.0740].
[53] G. Duplančić, S. Nabeebaccus, K. Passek-Kumerički, B. Pire, L. Szymanowski, and S. Wallon, Phys. Rev. D **107**, 094023 (2023).
[54] B. Pire, L. Szymanowski, and S. Wallon, Phys. Rev. D **101**, 074005 (2020); **103**, 059901(E) (2021).
[55] S. Scopetta, Phys. Rev. D **72**, 117502 (2005).
[56] B. Pasquini, M. Pincetti, and S. Boffi, Phys. Rev. D **72**, 094029 (2005).
[57] M. Pincetti, B. Pasquini, and S. Boffi, Czech. J. Phys. **56**, F229 (2006).
[58] D. Chakrabarti and C. Mondal, Phys. Rev. D **92**, 074012 (2015).
[59] D. Chakrabarti, R. Manohar, and A. Mukherjee, Phys. Rev. D **79**, 034006 (2009).
[60] H. Dahiya and A. Mukherjee, Phys. Rev. D **77**, 045032 (2008).
[61] N. Kumar and H. Dahiya, Phys. Rev. D **91**, 114031 (2015).
[62] G. R. Goldstein, J. O. Gonzalez Hernandez, and S. Liuti, arXiv:1401.0438.
[63] M. Gockeler, Ph. Hägler, R. Horsley, D. Pleiter, P. E. L. Rakow, A. Schäfer, G. Schierholz, and J. M. Zanotti (QCDSF Collaboration), Nucl. Phys. **A755**, 537 (2005).
[64] M. Gockeler, Ph. Hägler, R. Horsley, D. Pleiter, P. E. L. Rakow, A. Schäfer, G. Schierholz, and J. M. Zanotti (QCDSF and UKQCD Collaborations), Phys. Lett. B **627**, 113 (2005).
[65] D. Brommel, M. Diehl, M. Göckeler, Ph. Hägler, R. Horsley, Y. Nakamura, D. Pleiter, P. E. L. Rakow, A. Schäfer, G. Schierholz, H. Stüben, and J. M. Zanotti (QCDSF-UKQCD Collaborations), Prog. Part. Nucl. Phys. **61**, 73 (2008).
[66] M. Constantinou, R. Horsley, H. Panagopoulos, H. Perlt, P. E. L. Rakow, G. Schierholz, A. Schiller, and J. M. Zanotti, Phys. Rev. D **91**, 014502 (2015).
[67] H. W. Lin, E. R. Nocera, F. Olness, K. Orginos, J. Rojo, A. Accardi, C. Alexandrou, A. Bacchetta, G. Bozzi, J. W. Chen *et al.*, Prog. Part. Nucl. Phys. **100**, 107 (2018).

[68] M. Constantinou, A. Courtoy, M. A. Ebert, M. Engelhardt, T. Giani, T. Hobbs, T. J. Hou, A. Kusina, K. Kutak, J. Liang *et al.*, Prog. Part. Nucl. Phys. **121**, 103908 (2021).
[69] S. J. Brodsky and B. Q. Ma, Phys. Lett. B **381**, 317 (1996).
[70] X. Luan and Z. Lu, Phys. Lett. B **833**, 137299 (2022).
[71] A. Rajan, M. Engelhardt, and S. Liuti, Phys. Rev. D **98**, 074022 (2018).
[72] M. Diehl, Eur. Phys. J. C **19**, 485 (2001).
[73] S. J. Brodsky, M. Diehl, and D. S. Hwang, Nucl. Phys. **B596**, 99 (2001).
[74] G. P. Lepage and S. J. Brodsky, Phys. Rev. D **22**, 2157 (1980).
[75] B. W. Xiao and B. Q. Ma, Phys. Rev. D **68**, 034020 (2003).
[76] B. Pasquini and S. Boffi, Phys. Rev. D **73**, 094001 (2006).
[77] S. Kofler and B. Pasquini, Phys. Rev. D **95**, 094015 (2017).
[78] B. Pasquini and S. Boffi, Phys. Rev. D **76**, 074011 (2007).
[79] C. Zeng, H. Dong, T. Liu, P. Sun, and Y. Zhao, Phys. Rev. D **109**, 056002 (2024).
[80] M. Gluck, E. Reya, and A. Vogt, Z. Phys. C **53**, 651 (1992).
[81] A. D. Martin, W. J. Stirling, R. S. Thorne, and G. Watt, Eur. Phys. J. C **63**, 189 (2009).
[82] M. Diehl, Phys. Rep. **388**, 41 (2003).
[83] M. Burkardt, Phys. Lett. B **639**, 462 (2006).